CrossMark

ORIGINAL ARTICLE

Radiation risk index for pediatric CT: a patient-derived metric

Ehsan Samei[1,2,3] · Xiaoyu Tian[1] · W. Paul Segars[1,3] · Donald P. Frush[3,4]

Abstract

Background There is a benefit in characterizing radiation-induced cancer risk in pediatric chest and abdominopelvic CT: a singular metric that represents the whole-body radiation burden while also accounting for age, gender and organ sensitivity.

Objective To compute an index of radiation risk for pediatric chest and abdominopelvic CT.

Materials and methods Using a protocol approved by our institutional review board, 42 pediatric patients (age: 0-16 years, weight: 2-80 kg) were modeled into virtual whole-body anatomical models. Organ doses were estimated for clinical chest and abdominopelvic CT examinations of the patients using validated Monte Carlo simulations of two major scanner models. Using age-, size- and gender-specific organ risk coefficients, the values were converted to normalized effective dose (by dose length product) (denoted as the *k* factor) and a normalized risk *index* (denoted as the *q* factor). An analysis was performed to determine how these factors are correlated with patient age and size for both males and females to provide a strategy to better characterize individualized risk.

Results The *k* factor was found to be exponentially correlated with the average patient diameter. For both genders, the *q* factor also exhibited an exponential relationship with both the average patient diameter and with patient age. For both factors, the differences between the scanner models were less than 8%.

Conclusion The study defines a whole-body radiation risk index for chest and abdominopelvic CT imaging, that incorporates individual estimated organ dose values, organ radiation sensitivity, patient size, exposure age and patient gender. This indexing metrology enables the assessment and potential improvement of chest and abdominopelvic CT performance through surveillance of practice dose profiles across patients and may afford improved informed communication.

Keywords Children · Computed tomography · Effective dose · Radiation dose · Radiation risk

✉ Donald P. Frush
donald.frush@duke.edu

1 Department of Radiology,
Carl E. Ravin Advanced Imaging Laboratories,
Duke University Medical Center,
Durham, NC, USA

2 Department of Biomedical Engineering,
Electrical and Computer Engineering,
Duke University Medical Center,
Durham, NC, USA

3 Medical Physics Graduate Program,
Duke University Medical Center,
Durham, NC, USA

4 Division of Pediatric Radiology,
Department of Radiology,
Duke University Medical Center,
1905 McGovern-Davison Children's Health Center,
Durham, NC 27710, USA

Introduction

The number of computed tomography (CT) examinations in the United States and the resultant radiation exposure (and concern of radiation-induced cancer) have increased during the last 20 years, including in children [1–7]. As a result, it is recognized that dose to the pediatric population from CT scans should be closely managed [8] through exposure metrics.

In CT exposure metrology (the scientific process of quantifications of an attribute in numerical terms), there is a host of metrics as tabulated in Table 1. Each metric provides a different representation of contributing factors to CT radiation risk.

Table 1 Summary of the attributes and incorporating factors of currently available metrics for CT radiation exposure

	CTDI	SSDE	Organ dose	Effective dose	Effective risk
Physical quantity	●	⊙	⊙		
Derived quantity				●	●
Accounting for:					
Scanner model	●	●	●	●	●
Protocol parameters	●	●	●	●	●
Patient size		●	⊙	⊙	⊙
Organ-level dose			●	⊙	⊙
Patient age			⊙		●
Patient gender			⊙		●
Patient total radiation burden				●	●

● Yes – accounted for, ⊙ Possibly – depending on the implementation

CTDI CT dose index, *SSDE* size-specific dose estimate

Each also has its own limitations. Volume CT dose index–volume (CTDIvol) is a metric of the radiation output of a CT system but does not reflect the actual patient dose [9]. The size-specific dose estimate (SSDE) adjusts the scanner output by the patient's overall size but does not account for the patient's anatomical attributes such as body shape, organ location and orientation, and tissue composition [10]. Organ dose offers a notable advantage of addressing both the effect of scanner output and patient characteristics by compartmentalizing the CT irradiation burden. Prior efforts have sought to even personalize organ dose estimates [11]. However, while this level of granularity may be insightful and useful in many situations, it fails to provide a *single* value reflecting the patient's *whole-body* radiation burden, what is clinically most needed to represent the radiation burden from the examination. Effective dose meets this singularity requirement. However, it only provides a generic estimate of radiation risk [12, 13]. Technically defined for only a single reference phantom [14], conventional estimates of effective dose are based on tables that are not representative of the actual patient. The effective dose estimate, by definition, further ignores patient gender, size and age, factors that are known to markedly impact radiation risk and are of significant relevance to the pediatric population. Moreover, while characterizing radiation burden as radiation *dose* is most common, what is more relevant to dialogues with referring health care providers, patients and families is radiation *risk* [3, 6, 15, 16]. This need is so prevalent that in the absence of ascribing a radiation risk to an exam, the other alternatives (such as the CTDI) are by commission, omission or implication assumed to be proportional to the risk of the examination.

One reason for avoiding risk characterization is the difficulty in quantifying radiation risk associated with CT examinations in a useful manner. To begin to address some of the challenges with risk, the metric of effective risk, first introduced by Brenner [17], defined a weighted sum of equivalent doses to different tissues adopting weighting factors for the lifetime radiation-attributable tissue specific cancer risks per unit equivalent dose from the Biological Effects of Ionizing Radiations VII (BEIR VII) report [7]. The concept of effective risk can incorporate the effect of patient age and gender and as such addresses many limitations of other metrics. However, its implementation requires the knowledge of organ doses for a given CT scan. A rapid and accurate organ dose estimation generally requires either Monte Carlo simulations [18] or physical measurements [19] using anthropomorphic or computational models similar to the patient, challenges that are not practicable in a clinical setting. Furthermore, the use of the word "effective" as an adjective implies that we actually *know* what the risk to an individual patient is. In reality, risk to an individual patient is impacted by not only age and gender, but also other factors including the patient's genetic makeup. Furthermore, being mostly based on atomic bomb survivors, there are strong limitations in applying BEIR coefficients to partial and low irradiation conditions and differing population cohorts [20]. The uncertainties of any BEIR-based estimation will be large and, as such, it is more appropriate to characterize risk for an individual patient exposure as an *index* of the risk and not its effective value, in the same way that CTDI is an *index* of CT dose and not the actual CT dose.

Given the previously noted limitations of existing metrics, the purpose of this investigation was to provide a radiation risk estimation methodology and metric, incorporating important factors that affect radiation risk: organ dose, patient size, exposure age and gender. This novel metric is denoted as the risk *index* as an attempt to acknowledge the exact nature and limitation of the metrology. The study focused on common pediatric CT scans (chest and abdominopelvic scans) [21]. Using diverse pediatric patient models and Monte Carlo simulations, organ doses were estimated and used as a basis to estimate effective dose and the age-, size- and gender-specific risk *indices*. The effective doses and risk *indices* were normalized

by dose length product (DLP) to provide coefficients to enable convenient radiation risk indexing for a given pediatric CT examination in a way that is largely independent of the scanner model.

Materials and methods

Our institutional review board determined that the study was in compliance with the Health Insurance Portability and Accountability Act and did not require informed consent.

This study was partially funded by the National Institutes of Health. The authors had complete control over the data and information submitted in this article.

Patient-specific virtual models

Forty-two pediatric patients (age range: 0-16 years, weight range: 2-80 kg) consisting of 24 males (age range: 0-12 years, weight range: 2-80 kg) and 18 females (age range: 0-16 years, weight range: 2-41 kg) were included in the study. The cases were retrospectively identified from the patient database to represent anatomy of normal morphology and a wide and even sample of age and weight percentiles at our institution.

A whole-body computational model was created based on clinical CT images of each patient [22–24]. For each patient, the large organs were semiautomatically segmented. Each organ surface was initially defined as hundreds of three-dimensional triangulated polygon surfaces. A 3-D fitting program (Rhinoceros; McNeel North America, Seattle, WA) was subsequently deployed to reformat the organ surface into a 3-D non-uniform rational B-spline (NURBS) surface. The remainder of the patient anatomy was formed using existing male and female Visible Human adult models as templates morphed into the geometrical definitions of the segmented organs. The outcome of this process was validated as anatomical accuracy based on the reference standards of International Commission on Radiological Protection (ICRP) Publication 89 [25].

Organ dose estimation

Chest and abdominopelvic scans were simulated based on existing size-based pediatric protocols used clinically for each virtual model. Simulations were performed based on two commercial CT systems (A: LightSpeed VCT; GE Healthcare, Waukesha, WI; B: SOMATOM Definition Flash; Siemens Healthcare, Forcheim, Germany). Exact hardware features of each scanner were included in the simulations using a previously developed and validated Monte Carlo subroutine package for photon transport (PENELOPE, version 2006; Universitat de Barcelona, Spain) [26–28].

The full organ dose results are detailed in a companion publication [29]. In summary, simulations were based on clinically representative protocols (120 kVp, 38.4-40 mm collimation, 1.375-1.4 pitch for the two systems A-B, respectively). System A was assumed to deploy a small bowtie filter, while system B used a narrow bowtie filter. The chest protocol assumed imaging coverage from 1 cm above the lung apex to 1 cm below the lung base. The abdominopelvic protocol assumed imaging coverage from 1 cm above the top of the highest hemidiaphragm to 1 cm below the lowest aspect of the ischium. The total exposure length was assumed to include image coverage plus the over-ranging distance [30].

The energy deposited in the voxels confinement of each organ was summed and divided by organ mass to compute the organ dose. Some radiosensitive organs (e.g., salivary glands, oral mucosa and extrathoracic region) were not explicitly included in the organ dosimetry. For those organs, the dose values were assumed to match those of adjacent organs (pharynx and larynx).

Effective dose estimation

Equivalent organ doses, appropriately weighted and summed, can be converted to effective dose as

$$E_{ref} = \sum_T w_T H_t, \qquad (1)$$

where H_T is the calculated average dose to organ/tissue T of a single ICRP reference phantom, and w_T is the corresponding tissue weighting factor reflective of average radiosensitivities across genders and ages [14]. The use of a reference phantom, and thus the notation of E_{ref}, was intended to make effective dose applicable for estimating risk for radiation personnel generically, and not to patient dose. However, in the absence of other anthropomorphic whole-body metrics of radiation burden to patients, many investigators, practitioners and government agencies have adopted effective dose to patient dosimetry. In this work, we similarly computed effective dose for individual patients by using the summation of individual computed organ doses determined from individual virtual models. We denote this computation of effective dose as E_{pat} to make it distinct from that of the classical definition of the quantity. To make the values reflective of the patient gender, gonadal dose was assumed to be the dose to testes and ovaries for male and female models, respectively. The dose to the remainder tissues of each gender was averaged and ascribed to the "remainder" dose, and the dose to the breast was included for both genders.

Risk *index* estimation

For each patient model, the radiation burden was characterized as a risk *index* incorporating the impact of age and gender. The risk index was computed as a weighted sum, similar to the method used for effective dose [17] but with organ weighting

factors, r_{TGA}, that are tissue-(T), gender-(G) and age-(A) specific as

$$RI = \sum_T r_{TGA} H_T, \qquad (2)$$

The weighting factors were tissue-specific risk coefficients for lifetime attributable risk of cancer incidences interpolated from BEIR VII (from table 12D-1, BEIR VII) for discrete ages [7]. The risk coefficients for males included lung, liver, stomach, bladder, colon, prostate, thyroid, leukemia and other. The risk coefficients for females included breast, lung, liver, stomach, bladder, colon, thyroid, leukemia, ovary, uterus and other. The method used r_{other} risk coefficient for radiosensitive organs not listed in the reference. Those included the small intestine, bone surface, heart, gallbladder, kidney, pancreas, spleen, thymus, adrenal glands, oral mucosa, salivary glands, esophagus, lymph node, extrathoracic region, muscle, testes, skin and brain. For remaining organs (H_{other}), a method similar to that used for effective dose was applied [26]. The weighting factors were adopted from ICRP [14].

Data analysis

In order to make the data generalizable across scans with different radiation output levels, both the effective dose and risk *index* values were normalized by the DLP, estimated for a CTDI phantom (16 cm, more applicable to pediatric exams). This resulted in k factor for DLP normalized effective dose, and q factor for DLP normalized risk index. The factors were related to average patient diameter and age using a nonlinear regression analysis through a statistical software tool (R, version 2.14.1, R Foundation, Vienna, Austria). The feasibility of exponential dependency between the factors and the patient size were explored as well as the coefficients of the associated functions. The generalizability of the k and q factors for the two CT systems were ascertained via the average and percentage differences in the k and q factors between scanners across the patient models.

Results

The k factor showed a strong exponential relationship with average patient diameter, as demonstrated in Figs. 1 and 2 for chest and abdominopelvic scans, respectively. Between the two scanner models, the average difference was below 8% (Tables 2 and 3). Since the differences were relatively small, the k factor was averaged across the two scanner models. The results were related to the average patient diameter as

$$k_{chest} = 0.5 \sum_S \frac{E_{pat,S}}{DLP_S} = \exp(\alpha_k d_{chest} + \beta_k), \qquad (3)$$
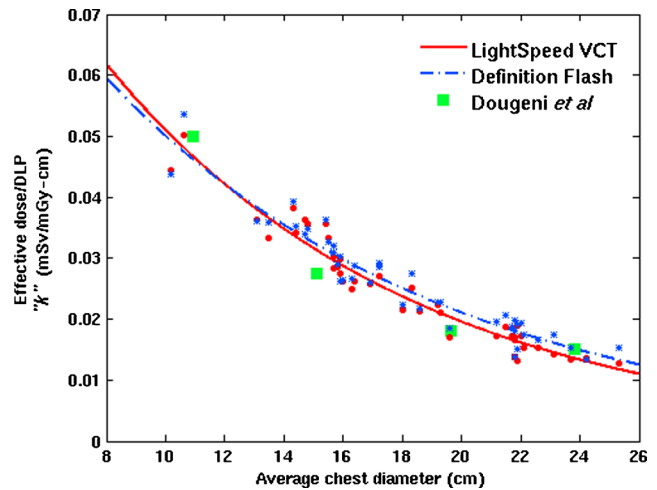

Fig. 1 Effective dose (normalized to dose length product [DLP], k factor) for chest scans as a function of patient average chest diameter. Green square = k factors measured by Dougeni et al. [31] using thermoluminescent dosimeter chips for reference pediatric phantoms at 0 (newborn), 1, 5 and 10 years of age. Protocol used in the study by Dougeni et al. [31]: 64-slice multidetector CT scanner, 120 kVp, 200 mAs, 10 mm slice thickness. The equations of the regression lines are according to Equation 3 and Table 2

and

$$k_{abd} = 0.5 \sum_S \frac{E_{pat,S}}{DLP_S} = \exp(\alpha_k d_{abd} + \beta_k), \qquad (4)$$

where $E_{pat,S}$ is effective dose specific to each scanner, and k is the normalized scanner-independent effective dose value. The fitting parameters α_k and β_k are reported in Tables 2 and 3 for chest and abdominopelvic scans, respectively.

The q factors similarly exhibited exponential relationships with patient diameter and with patient age for both males and females. The differences between scanners were again less than
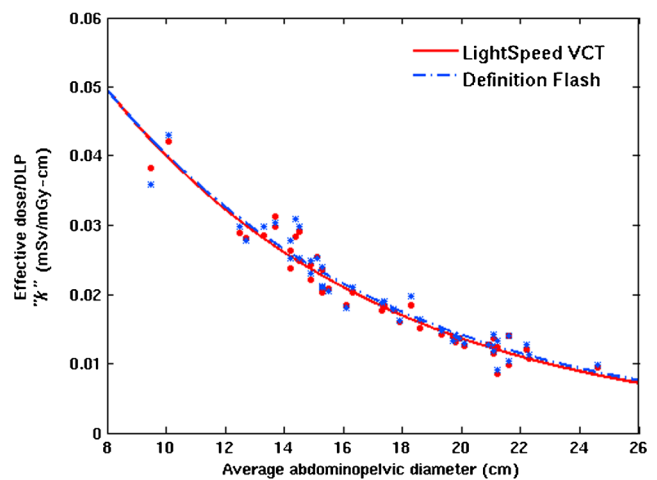

Fig. 2 Effective dose (normalized to dose length product [DLP], k factor) for abdominopelvic scans as a function of patient average abdominopelvic diameter. The equations of the regression lines are according to Equation 4 and Table 3

Table 2 Dose length product (DLP)-normalized effective dose (k factor) and DLP-normalized risk index (q factor) for chest scans as a function of chest diameter (Equations 3 and 5)

Conversion coefficients	α	β	γ	Correlation coefficient for the fits (R²)	Average difference between scanners (%)	Range of differences between scanners (%)
k factor	−0.090	−2.10	-	0.95	7.6	−22.6, 11.8
q factor (male)	−0.098	−0.056	3.37	0.99	5.5	−16.5, 15.4
q factor (female)	−0.059	−0.084	3.85	0.97	7.7	−24.0, 4.9

The unit for normalized risk index is cases per 1,000,000 exposed patients per milligray-centimeters. DLP was estimated using a 16-cm-diameter CT dose index phantom

8%. As such, the data were pooled across scanners and scanner-independent exponential regressions were established as

$$q_{chest} = 0.5 \sum_s \frac{RI_s}{DLP_S} = \exp\left(\alpha_q d_{chest} + \beta_q A + \gamma_q\right), \quad (5)$$

and

$$q_{abd} = 0.5 \sum_S \frac{RI_S}{DLP_S} = \exp\left(\alpha_q d_{abd} + \beta_q A + \gamma_q\right), \quad (6)$$

where RI_s is the risk index specific to each scanner, and q is the normalized scanner-independent risk index value. The fitting parameters α_q, β_q, and γ_q are tabulated in Tables 2 and 3 for chest and abdominopelvic scans, respectively.

Figures 3 and 4 illustrate the dependency of risk index to age and size for males and females. These illustrations are designed to depict multiple degrees of dependency in a single figure. The age is represented on the y-axis and size on the x-axis. The color contours reflect the magnitude of normalized risk index. Using the age and gender of a patient, the plots illustrate the associated risk index. The dotted lines represent 50th percentile males and females. The solid lines represent 5th and 95th percentiles. The data points represent individual patient models in the study.

Discussion

Characterizing the magnitude of CT radiation for an individual patient examination has emerged as an unavoidable requirement to practice medical imaging. This is now required

in California [33]. Patients are also increasingly asking for this information [34]. Furthermore, from a clinical as well as a scientific standpoint, there is a growing need to assess the magnitude of CT irradiation in units that are relevant and patient specific so that the imaging procedure can be individualized and appropriately optimized [35]. Current metrics of CT dose fall short of meeting many requirements that such a metric should ideally have (Table 1). In this work, we attempted to characterize a radiation risk metric for pediatric CT scans that incorporates the effects of many influencing factors on pediatric radiation risk: organ dose, organ radiation sensitivity, patient size, patient age and patient gender, all incorporating scanner specific information and patient specific anatomical geometries.

The risk estimation for CT scans is highly controversial and mainly criticized based on the hypotheses and uncertainties associated with risk coefficients and models at effective doses below 100 mSv [20]. While some have advocated the estimation of risk [17, 36], others have voiced major qualifications and concerns [36, 37]. Leading organizations including the American Association of Physicists in Medicine (AAPM) have released public statements highlighting the uncertainties associated with risk estimation at low exposure levels [38]. We fully acknowledge the limitations and uncertainties. Yet, in the face of uncertainty, we believe it is our obligation as health care professionals to take the path that affords the lowest amount of radiation burden needed while still appropriate so as to not compromise diagnostic performance, which is the primary purpose of the examination. It follows that implementing a reduction of radiation burden that is meaningful requires metrics that

Table 3 Dose length product (DLP)-normalized effective dose (k factor) and DLP-normalized risk index (q factor) for abdominopelvic scans as a function of abdominopelvic diameter (Equations 4 and 6)

Conversion coefficients	α	β	γ	Correlation coefficient for the fits (R²)	Average difference between scanners (%)	Range of differences between scanners (%)
k factor	−0.103	−2.194	-	0.95	3.6	−8.5, 5.8
q factor (male)	−0.095	−0.060	3.28	0.98	4.2	−9.2, 0
q factor (female)	−0.05	−0.114	3.05	0.96	7.3	−4.2, 13.0

The unit for normalized risk index is cases per 1,000,000 exposed patients per milligray-centimeters. DLP was estimated using a 16-cm-diameter CT dose index phantom

Fig. 3 The risk *index* (normalized by dose length product [DLP], *q* factor) dependency with age and average chest diameter for the two genders (left, right). Dotted points represent indices associated with individual patients. Dotted lines and solid lines represent mean chest diameter and the 95% prediction intervals, respectively, based on thorax size data for pediatric patients [32]
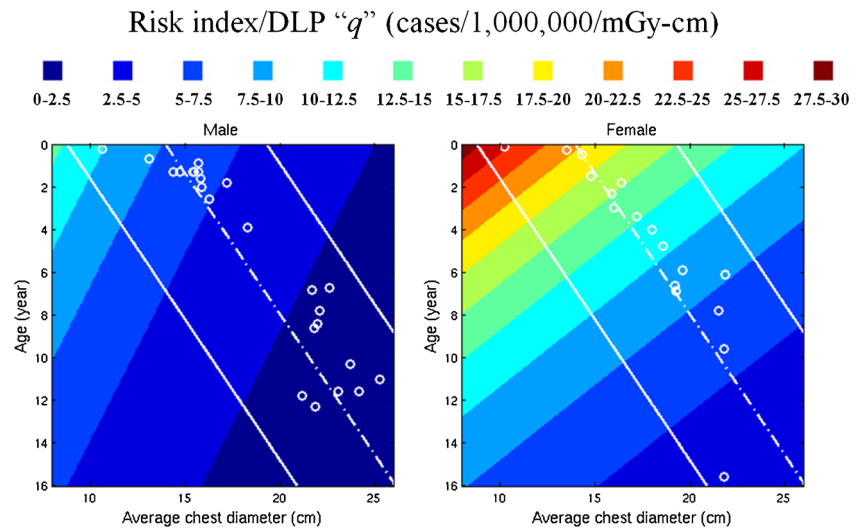
are relevant to potential harm. Otherwise, metrics of radiation output that have never been intended to be used as risk estimates for an individual patient, such as CTDI or even effective dose, would be taken as surrogates of risk implied to be linearly proportional to the individual's actual risk.

Our methodology to characterize dose does not address existing challenges associated with any risk estimation for medical imaging. Those include genetic disposition of patients, population-based risk estimation, uncertainties at low radiation levels, partial irradiation of certain organs and the applicability of the linear, no-threshold model [20]. However, our methodology accounts for some of the key factors that are *already* known to affect radiation risk but have been under-represented due to insufficient organ dose information. We adjusted for such determinants that are universally acknowledged among contributors to the CT risk debate [20, 39–41]: age, gender and organ sensitivity. Given the fact that these

determinants of risk are well recognized, it is certainly reasonable to allow their relevance to influence imaging optimization. In addressing challenges of risk, we further qualify our justification of risk quantification to state it as a risk *index*, acknowledging the limits of our knowledge based on available patient information and risk models and data.

The risk *index* metrology utilized in this work provides a convenient means by which an individual patient risk can be characterized in reference to a population risk similar in size, gender and age. We attribute our risk indexing to the "individual" in recognition that risk is at its core a population-based construct. Risk is always a population-based metric and as such, its ascription to an individual patient should never be interpreted deterministically. That is, the risk is not *assigned* to an individual; rather the individual by nature of the pertinent circumstances would best fit into that amount of risk defined

Fig. 4 The risk *index* (normalized by dose length product [DLP], *q* factor) dependency with age and average abdominal diameter for the two genders (left, right). Dotted points represent indices associated with individual patients. Dotted lines and solid lines represent mean abdominal diameter and the 95% prediction intervals, respectively, based on abdominal size data for pediatric patients [32]
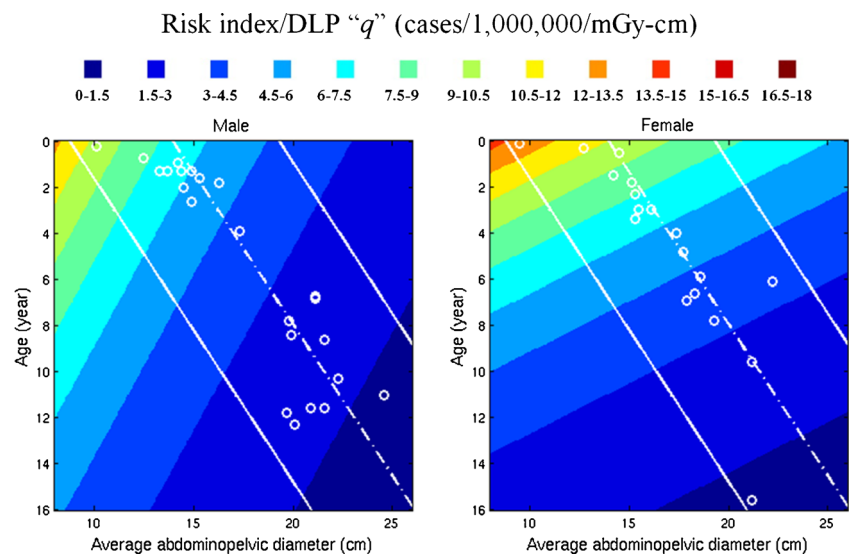
at a population level. For example, a 1/100 risk to an individual does not mean that she/he will experience 1/100th of the harm or see that effect 1 in 100 times, but that the harm level occurs at that rate in a similar population. The number in the denominator (100) in this individualized ascription already implies a *population*, a reference to which enables the estimation of risk.

As a practical example of how estimating effective dose and risk *index* using the k and q factors provided in this study can be used in the clinical setting, consider a 9-year, 4-month-old boy who undergoes an abdominopelvic CT examination. The 16-cm $CTDI_{vol}$ and DLP for the examination are 4.26 mGy and 180 mGy-cm, respectively. Given that child's average abdominopelvic diameter of 20.8 cm [32] and using the fitting parameters (Table 3), the effective dose associated with this scan may be determined as follows:

$$E_{pat} = DLP \times \exp(\alpha_k d_{abd} + \beta_k)$$
$$= 180 \times \exp(\text{-}0.103 \times 20.8 \text{-} 2.194)$$
$$= 12.35 \text{ mSv}$$

The risk *index* for cancer incidence is similarly estimated as follows:

$$RI = DLP \times \exp\left(\alpha_q d_{abd} + \beta_q A + \gamma_q\right)$$
$$= 180 \times \exp(\text{-}0.095 \times 20.8 \text{-} 0.060 \times 9.3 + 3.28)$$
$$= 1\ text/2,638\ exposed$$

As shown in the above example, the risk *index* for this particular CT exam (and in fact for the majority of CT exams) is extremely small compared to other risk factors and well in line with other imaging examinations [34, 42]. From our clinical practice, we have found the opportunity to effectively communicate the (small) amount of risk associated with a justified imaging exam provides a beneficial perspective for the patient as to how small the risk *might be* (emphasizing the indexing element of the risk quantification in reference to a population of like individuals) in comparison to the significant potential clinical benefits of such an exam. Nonetheless, providing an index to reflect some likelihood of harm allows means by which to potentially better understand all aspects (benefits and potential risks) of an examination. Conversely, not being able to speak to relevant patients and families/caregivers (recognizing that the need and circumstances for such will vary) about the risk or use metrics that are nonintuitive (e.g., CTDI) can be misunderstood as a lack of knowledge, a lack of transparency or a perception that the risk is higher than it actually is. This is also not a call to discuss risk in every scenario, but to have the ability for more accurate (e.g., using organ doses for effective dose determination) and relevant dialogues (risk as opposed to dose) when needed.

For chest scans, the k factor reported in our study is consistent with data from others. Dougeni et al. [31] utilized thermoluminescent dosimeters (TLD) to measure dose received by four pediatric anthropomorphic phantoms representing ages 0, 5, 10 and 15 years old. Our results were within 12% of those results as shown in Fig. 1. Our results are further generally consistent with earlier work by Alessio and Phillips [40] but with additional provisions in the current study for both patient age and size to be independent input parameters. This was made possible by the variability in the atlas of the patient models deployed in the study. In terms of effective dose comparisons, we again acknowledge that effective dose estimated in this study does not follow the ICRP definition [14] based on a *hermaphrodite* reference phantom. In fact, the concept is stated as being only applicable to assess radiation burden to radiation workers. However, current medical literature and guidelines frequently use effective dose to state the radiation dose to a patient [43]. This use is primarily due to the lack of a better existing metric to compare individual radiation burdens across imaging modalities or with background exposures.

Certain limitations of this study are noted. While these data are generalized to two widely used CT systems and representative protocols, their applicability to other systems and varying protocols (and kVp) would require verification. The study further included only body protocols. The investigation could be extended to other examinations including those of extremities, brain or cervical spine. The risk model used was based on lifetime attributable risk of cancer incidence, not mortality. Mortality-based risk requires additional information and conversion factors. This study also pertained only to estimates/indices for dose and risk of CT exams and not their benefit [44], a topic that requires a thorough methodology and study of its own.

Conclusion

In this study, we implemented whole-body radiation risk metrics for pediatric chest and abdominopelvic CT scans. These metrics, when normalized by DLP, show a strong exponential relationship with patient characteristic (age and size), with small differences between the two scanner models. The reported correlation relationships can be used to more efficiently and accurately characterize risk when needed in clinical practice for pediatric body CT. The methodology also provides a perspective more closely aligned with risk than current CT dose metrics for dose optimization and protocol design.

Compliance with ethical standards

Conflicts of interest None.

References

1. Bahador B (1996) Trends in diagnostic imaging to 2000. Urch Publishing, London
2. IMV (2012) CT Market Outlook Report. IMV Medical Information Division, Des Plaines, IL
3. Brenner DJ, Hall EJ (2007) Computed tomography–an increasing source of radiation exposure. N Engl J Med 357:2277–2284
4. McCollough CH, Chen GH, Kalender W et al (2012) Achieving routine submillisievert CT scanning: report from the summit on management of radiation dose in CT. Radiology 264:567–580
5. Goske MJ, Applegate KE, Boylan J et al (2008) The image gently campaign: working together to change practice. AJR Am J Roentgenol 190:273–274
6. Pearce MS, Salotti JA, Little MP et al (2012) Radiation exposure from CT scans in childhood and subsequent risk of leukaemia and brain tumours: a retrospective cohort study. Lancet 380:499–505
7. National Research Council (2006) Health risks from exposure to low levels of ionizing radiation — BEIR VII. The National Academies Press, Washington, DC
8. Goske MJ, Applegate KE, Boylan J et al (2008) Image gently(SM): a national education and communication campaign in radiology using the science of social marketing. J Am Coll Radiol 5:1200–1205
9. McCollough CH, Leng S, Yu L et al (2011) CT dose index and patient dose: they are not the same thing. Radiology 259:311–316
10. AAPM (2011) Size-specific dose estimates (SSDE) in pediatric and adult body CT examinations, AAPM report no. 204. American Association of Physicists in Medicine, College Park, MD
11. Kalender WA (2014) Dose in x-ray computed tomography. Phys Med Biol 59:R129–R150
12. Martin CJ (2007) Effective dose: how should it be applied to medical exposures? Br J Radiol 80:639–647
13. McCollough CH, Christner JA, Kofler JM (2010) How effective is effective dose as a predictor of radiation risk? AJR Am J Roentgenol 194:890–896
14. International Commission on Radiological Protection (2007) The 2007 recommendations of the international commission on radiological protection, ICRP publication 103. Essen, Germany
15. Bogdanich W (2009) Radiation overdoses point up dangers of CT scans. In the New York Times. Available at: http://www.nytimes.com/2009/10/16/us/16radiation.html
16. Bogdanich W (2011) West Virginia hospital over radiated brain scan patients, records show. In the New York Times. Available at: http://www.nytimes.com/2011/03/06/health/06radiation.html?_r=3
17. Brenner DJ (2008) Effective dose: a flawed concept that could and should be replaced. Br J Radiol 81:521–523
18. Lee C, Lee C, Staton RJ et al (2007) Organ and effective doses in pediatric patients undergoing helical multislice computed tomography examination. Med Phys 34:1858–1873
19. Hurwitz LM, Reiman RE, Yoshizumi TT et al (2007) Radiation dose from contemporary cardiothoracic multidetector CT protocols with an anthropomorphic female phantom: implications for cancer induction. Radiology 245:742–750
20. Hendee WR, O'Connor MK (2012) Radiation risks of medical imaging: separating fact from fantasy. Radiology 264:312–321
21. Dorfman AL, Fazel R, Einstein AJ et al (2011) Use of medical imaging procedures with ionizing radiation in children: a population-based study. Arch Pediatr Adolesc Med 165:458–464
22. Li X, Samei E, Segars WP et al (2011) Patient-specific radiation dose and cancer risk estimation in CT: part II. Application to patients. Med Phys 38:408–419
23. Segars WP, Mahesh M, Beck TJ et al (2008) Realistic CT simulation using the 4D XCAT phantom. Med Phys 35:3800–3808
24. Segars WP, Sturgeon G, et al (2009). Patient specific computerized phantoms to estimate dose in pediatric CT. SPIE Proceedings, p 72580H
25. ICRP (2002) Basic anatomical and physiological data for use in radiological protection: reference values, ICRP publication 89. International Commission on Radiological Protection, New York
26. Baro J, Sempau J, Fernandez-Varea JM, Salvat F (1995) PENELOPE: an algorithm for Monte Carlo simulation of the penetration and energy loss of electrons and positrons in matter. Nucl Instrum Meth B 100:31–46
27. Sempau J, Fernandez-Varea JM, Acosta E, Salvat F (2003) Experimental benchmarks of the Monte Carlo code PENELOPE. Nucl Instrum Meth B 207:107–123
28. Li X, Samei E, Segars WP et al (2011) Patient-specific radiation dose and cancer risk estimation in CT: part I. Development and validation of a Monte Carlo program. Med Phys 38:397–407
29. Tian X, Li X, Segars WP et al (2014) Pediatric chest and abdominopelvic CT: organ dose estimation based on 42 patient models. Radiology 270:535–547
30. Li X, Samei E, Segars WP et al (2011) Patient-specific radiation dose and cancer risk for pediatric chest CT. Radiology 259:862–874
31. Dougeni E, Chapple CL, Willis J et al (2011) Assessment of effective dose in paediatric CT examinations. Radiat Prot Dosim 147:147–150
32. Kleinman PL, Strauss KJ, Zurakowski D et al (2010) Patient size measured on CT images as a function of age at a tertiary care children's hospital. AJR Am J Roentgenol 194:1611–1619
33. The State of California SB 1237 (2010) Available at: http://www.leginfo.ca.gov/pub/09-10/bill/sen/sb_1201-1250/sb_1237_bill_20100929_chaptered.html
34. Hendrick RE, Dodd GD 3rd, Fullerton GD et al (2012) The University of Colorado Radiology Adult Dose-Risk Smartcard. J Am Coll Radiol 9:290–292
35. The Joint Commission (2011) Sentinel Event Alert, Issue 47, Aug 24, 2011
36. Dietze G, Harrison JD, Menzel HG (2009) Effective dose: a flawed concept that could and should be replaced. Comments on a paper by D J Brenner (Br J Radiol 2008;81:521-3). Br J Radiol 82:348–350 author reply 350-341
37. Pradhan AS, Kim JL, Lee JI (2012) On the use of "effective dose" (E) in medical exposures. J Med Phys 37:63–65
38. American Association of Physicists in Medicine (2011). AAPM position statement on radiation risks from medical imaging procedures Available at http://www.aapm.org/org/policies/details.asp?id=318&type=PP
39. Brenner DJ, Hall EJ (2012) Cancer risks from CT scans: now we have data, what next? Radiology 265:330–331
40. Alessio AM, Phillips GS (2010) A pediatric CT dose and risk estimator. Pediatr Radiol 40:1816–1821
41. Colagrande S, Origgi D, Zatelli G et al (2014) CT exposure in adult and paediatric patients: a review of the mechanisms of damage, relative dose and consequent possible risks. Radiol Med 119:803–810
42. Peck DJ, Samei E (2017) American College of Radiology: How to understand and communicate radiation risk. http://www.imagewisely.org/imaging-modalities/computed-tomography/medical-physicists/articles/how-to-understand-and-communicate-radiation-risk. Accessed 07 Aug 2017
43. Deak PD, Smal Y, Kalender WA (2010) Multisection CT protocols: sex- and age-specific conversion factors used to determine effective dose from dose-length product. Radiology 257:158–166
44. Fletcher JG, Kofler JM, Coburn JA et al (2013) Perspective on radiation risk in CT imaging. Abdom Imaging 38:22–31